Princeton Plasma Physics Laboratory

PPPL-4202

PPPL-4202

Recent Developments in Electron Cyclotron Emission Research on Magnetically Confined Plasmas

Gary Taylor

December 2006

PPPL
PRINCETON PLASMA PHYSICS LABORATORY

Prepared for the U.S. Department of Energy under Contract DE-AC02-76CH03073.

Princeton Plasma Physics Laboratory
Report Disclaimers

Full Legal Disclaimer

Trademark Disclaimer

PPPL Report Availability

Princeton Plasma Physics Laboratory:

http://www.pppl.gov/pub_report/

Office of Scientific and Technical Information (OSTI):

http://www.osti.gov/bridge

U.S. Department of Energy:

U.S. Department of Energy
Office of Scientific and Technical Information
P.O. Box 62
Oak Ridge, TN 37831-0062
Telephone: (865) 576-8401
Fax: (865) 576-5728
E-mail: reports@adonis.osti.gov

RECENT DEVELOPMENTS IN ELECTRON CYCLOTRON EMISSION RESEARCH ON MAGNETICALLY CONFINED PLASMAS

Gary Taylor

Princeton Plasma Physics Laboratory, Princeton University,

Princeton, New Jersey 08543, USA

Abstract

Electron cyclotron emission (ECE) has been an important diagnostic for measuring the temporal evolution of the electron temperature profile in magnetically confined plasma devices for more than 25 years. Recent advances in ECE measurements, such as 2-D ECE imaging and ECE intensity correlation techniques, have provided detailed information on sawtooth reconnection, neoclassical tearing mode behavior, electron heat transport, fast electron dynamics, and fast particle-driven Alfvén eigenmodes. ECE spectral analysis is benefiting from improved ECE modeling and significant increases in computational power that allow fast, real-time, temperature measurements. Mode-converted electron Bernstein wave emission (EBE) diagnostics are being developed to study overdense ($\omega_{pe} >> \omega_{ce}$) plasmas, a regime where conventional ECE diagnostics cannot be applied and one commonly encountered in high β devices, such as the spherical torus and reversed-field pinch. While ECE diagnostic techniques are now well established on many existing magnetically confined plasmas, significant challenges lie ahead for applying ECE techniques to reactor-grade plasmas, such as ITER where $T_e(0)$ is expected to reach 20-40 keV. This paper reviews the recent advances in ECE, electron cyclotron absorption and EBE diagnostics and discusses the challenges for ECE measurements on ITER.

I. INTRODUCTION

The measurement of electron cyclotron emission (ECE) from magnetically confined plasmas has been an important diagnostic technique for studying the temporal evolution of the electron temperature profile ($T_e(R,t)$) for more than a quarter-century. Electron cyclotron emission (ECE) radiates from plasma confined in a magnetic field as the electrons spiral around the magnetic field. ECE is radiated at the electron cyclotron frequency, $\omega_{ce} = eB/\gamma m_e$ and its harmonics, where e is the electronic charge, B is the magnetic field strength, m_e is the electron mass and γ is the Lorentz relativistic mass factor [1]. Confining magnetic fields used in nuclear fusion research are typically in the range of 0.5-10 T, so that ECE is emitted in the 10-500 GHz frequency band. In most devices used for magnetically confined nuclear fusion research, ECE at the fundamental EC frequency with ordinary mode (O-mode) polarization and the second harmonic EC frequency with extraordinary mode (X-mode) polarization is at blackbody levels. $T_e(R,t)$ is measured by detecting this blackbody-level ECE along a magnetic field gradient.

The first ECE spectral measurements on a tokamak were made in the early 1970s [2] and the potential for using ECE spectra to diagnose plasmas was suggested at about the same time [3, 4]. Much of the ECE research in the 1970's was directed towards understanding the physical processes that affect the ECE spectrum, such as wall reflections in optically thin plasmas and mode mixing between O-mode and X-mode polarizations [5, 6]. O-mode polarized radiation at fundamental ECE frequencies was found to be at the blackbody level in the Princeton Large Tokamak (PLT) [7] and the measured ECE optical depth on PLT agreed with hot-plasma theory [8]. By the early 1980's ECE had been established as a standard $T_e(R,t)$ diagnostic on many magnetically confined plasma devices used for nuclear fusion research. BORNATICI et al. [9]

published an excellent review of ECE research and its diagnostic potential during this early period of development.

During the past 25 years there has been significant theoretical research on ECE from non-thermal, anisotropic electron distributions [10] and on the effect of non-thermal distributions on electron temperature measurements [11]. ECE diagnostics have studied the complex spatial and temporal evolution of fast magneto-hydrodynamic (MHD) instabilities [12, 13] and electron temperature fluctuations [14]. Vertically [15] and obliquely [16] viewing ECE systems have studied the generation and transport of energetic non-thermal electrons. In optically thin plasmas, electron cyclotron absorption (ECA), combined with an independent measurement of density, has been used to measure electron temperature [17] while being relatively insensitive to non-thermal emission. ECA has also yielded valuable information on the electron distribution function [18].

A relatively recent development is the use of mode-converted electron Bernstein wave emission (EBE) to study overdense ($\omega_{pe} >> \omega_{ce}$) plasmas, a regime where conventional ECE diagnostics cannot be applied and that is characteristic of high β devices, such as the spherical torus and reversed-field pinch. EBE can mode-convert to electromagnetic radiation outside the plasma, by either coupling to the X-mode (B-X conversion) [19] or to the O-mode (B-X-O conversion) [20]. After mode conversion conventional microwave radiometry techniques can be employed. $T_e(R,t)$ was first measured successfully with EBE radiometry, via B-X-O conversion, on the Wendelstein 7-AS stellarator (W7-AS) [21, 22]

ECE diagnostic systems fall into two classes; quasi-optic instruments including the Martin-Puplett Michelson interferometer [23-25] and the multi-channel grating

polychromator [26, 27], and instruments that employ microwave techniques, such as fast frequency scanning and multi-channel heterodyne radiometers [28-30]. Michelson ECE instruments have a large throughput, enabling absolute calibration and they are well suited to broadband ECE studies of non-Maxwellian electron behavior. During the past 10-15 years, heterodyne radiometry has benefited from major advances in millimeter wave technology and microwave system integration. The temporal and spatial resolution of heterodyne systems is generally far superior to quasi-optic instruments, allowing heterodyne ECE diagnostics to be used in the study of fast phenomena such as energetic particle-driven modes and turbulent fluctuations [14, 31]. A review of heterodyne radiometry techniques was published by HARTFUSS, et al. [32] in the late 1990's.

This paper will review developments in ECE, ECA and EBE research that have occurred during the past 5 years. Many of the most recent papers referenced in this review were either originally presented at the 14th *Joint Workshop on ECE and ECRH* that was held in May 2006 on Santorini Island in Greece, or appear in this issue of *Fusion Science and Technology*. This review covers a period when ECE measurements have provided detailed information on sawtooth reconnection, electron heat transport, fast electron dynamics, and fast particle-driven modes. ECE spectral analysis is now clearly benefiting from the confluence of significantly improved numerical modeling and ubiquitous, inexpensive computer systems. These technical developments have, for example, allowed ECE diagnostics to provide fast, real-time, $T_e(R,t)$ measurements for plasma feedback systems. Looking towards the future, as the electron temperature in magnetically confined plasmas rises well beyond 10 keV, relativistic effects will become increasingly important. The large relativistic downshift and spectral broadening characteristic of plasmas in this high T_e regime shifts the emitting layer and results in

increased harmonic overlap that constrains radial access and degrades radial resolution. These issues will only become more challenging as magnetically confined nuclear fusion research moves to reactor-grade plasmas, such as ITER, where T_e is expected to reach 20-40 keV.

Section II of this paper describes developments in ECE-related technology and Section III presents some recent results from ECE and ECA measurements. Section IV discusses important advances in 2-D ECE imaging and how this relatively new technique is changing our understanding of magnetic reconnection physics. Section V reviews recent developments in EBE research on overdense plasmas and Section VI discusses future challenges for ECE measurements on ITER.

II. DEVELOPMENTS IN ECE RELATED TECHNOLOGY

The standard ECE Martin-Puplett, Michelson interferometer [23-25] has undergone significant improvements in recent years. The development of the rotating mirror Michelson interferometer has allowed up to six input channels, and mirror scan times that are at least an order of magnitude faster than conventional reciprocating mirror Michelson interferometers. The rotating helicoidal mirror Michelson interferometer design originally employed on FTU [33] has been extended to allow for simultaneous ECE measurements on six channels [34, 35]. The spectrometer is now installed on the Joint European Torus (JET) tokamak in England, where it will provide simultaneous measurements in two polarizations via one perpendicular and two oblique views (Fig. 1) [36]. The helicoidal mirror in the Michelson interferometer has four steps (Fig. 2) and revolves at 1400 rpm, giving a scan time of 10.7 ms. The diagnostic detects ECE between 75 and 400 GHz with 7.5 GHz spectral resolution, resulting in a major radial resolution of better than 10 cm.

ECE $T_e(R)$ measurements are increasingly being used to provide real-time feedback signals. On the Tore-Supra tokamak in Cadarache, France, a 32-channel ECE radiometer provides real-time $T_e(R)$ feedback for controlling the transport barrier in steady-state lower hybrid current drive (LHCD) discharges [37]. $T_e(R)$ is generated from ECE data every millisecond by using analytic expressions to radially map the ECE spectra. The radial mapping uses magnetic equilibrium data and the electron density to calculate paramagnetic and diamagnetic field corrections. The relativistic frequency shifts are also estimated in real-time. The processing time for each $T_e(R)$ time slice is 600 μs. Good agreement is obtained between the real time system and the post-shot analysis.

Neoclassical Tearing Mode (NTM) suppression by electron cyclotron resonance heating (ECRH) or electron cyclotron current drive (ECCD) requires the deposition profile to be precisely aligned at the location of the NTM in order to achieve efficient stabilization. NTM suppression may be critical on ITER and dedicated ECE systems are being developed to provide feedback control for NTM suppression systems. A "line-of-sight" feedback system has been designed for installation on the TEXTOR tokamak in Jülich, Germany [38]. Figure 3(a) shows a schematic of the feedback system. An 800 kW, 140 GHz 10 s gyrotron transmission line has a Fabry-Perot frequency selective coupler (FSC) installed in it that is transparent to the gyrotron frequency but reflective to frequencies that are nearby. The reflected ECE is transported to a six channel heterodyne radiometer, operating between 132.5 and 147.5 GHz. Because the ECE signal contains significant levels (~ 100 W) of stray gyrotron power reflected from the walls of the tokamak an 11 orders of magnitude attenuation of the stray signal is required before the ECE is detected by the radiometer. In order to accomplish this a second FSC is used to attenuate the stray gyrotron radiation at the input to the

radiometer (Fig. 3(b)). With this additional FSC and a notch filter the stray power is comparable to the ECE and does not saturate the input to the radiometer.

ECE measurements oblique to the confining magnetic field direction can be a powerful tool for studying non-Maxwellian electron distributions. Emission at different oblique angles comes from electrons having different velocities. On the TCV tokamak in Lausanne, Switzerland, a real-time steered obliquely-viewing ECE radiometer has been installed and used to measure non-thermal ECE during ECCD [39]. The radiometer uses a modified ECRH launcher that can be rapidly steered over 45 degrees in 500 ms. Preliminary measurements during ECRH and ECCD plasmas, with the system cross-calibrated to Thomson scattering during an ECRH discharge, showed indications of non-thermal emission during low power (250 kW) ECCD.

A new antenna dedicated to oblique ECE measurements has been installed recently on the compact FTU tokamak in Frascati, Italy, where it will be used to study non-thermal electrons generated during LHCD [40]. The compact nature of FTU and the fact that it is also liquid-nitrogen cooled and surrounded by a cryostat, means that it is difficult to design an ECE system with an oblique view. Vignetting by the wall of the tall and narrow vertical viewport limits the maximum angle between the line-of-sight and the perpendicular to the magnetic field to 20^{o} at the plasma edge and to 30^{o} at the plasma axis. This limits the diagnostic to being sensitive to electrons with energies below 15 keV. A 12-channel grating polychromator is connected to the antenna to measure optically thin X-mode polarized ECE from the antenna. In order to remove O-mode emission that is close to blackbody due to reflections, a quarter-wave plate is used to transform the oblique, elliptically polarized, emission to linear polarization that can then be filtered with a wire grid.

ECE diagnostics often require vacuum windows with low attenuation and reflectivity over a wide frequency band. This is normally accomplished by adding dielectric coatings of suitable permittivity and thickness. Coatings on the vacuum side must be vacuum compatible and resistant to plasma radiation. Recently, a rugged multilayer vacuum window design has been developed for wide-band microwave plasma diagnostics that satisfies these requirements [41]. A boron nitride disk was installed on the vacuum side of a fused silica window and a layer of Teflon was added to the atmospheric pressure side. This multi-layer window attained a power reflection coefficient as low as 0.025 in the 26.5–40, 40–56, and 56–75 GHz frequency bands and as low as 0.01 in the 75–92 and 92–110 GHz frequency bands.

As data analysis, modeling, and computing networks become increasingly fast, complex new integrated approaches to data analysis on fusion research devices become possible. For example, on the steady-state Wendelstein 7-X (W7-X) stellarator, being constructed at Greifswald in Germany, a vast amount of strongly-linked plasma diagnostic data, including ECE spectra, will be continuously analyzed to benchmark the plasma behavior against physics models [42]. Within this context, the approach being followed in order to analyze the ECE data is to fit the ECE spectra obtained by both low field side (LFS) and high field side (HFS) antennas in both the "bean-shaped" and "triangular" sections of W7-X with a simulated model spectrum that includes the antenna pattern, receiver characteristics etc. [43]. On W7-X, the primary ECE $T_e(R)$ diagnostic will be a second harmonic, X-mode radiometer that will be installed on the LFS of one of the "bean-shaped" sections where the major radial magnetic field gradient is large. Additional non-thermal electron information can be obtained from HFS measurements in both the "bean-shaped" and "triangular" sections. ECE from ripple

trapped electrons in the "triangular" sections can contribute 50% of the ECE signal as compared to less than 15% of the ECE signal from the "bean-shaped" sections.

III. RECENT ECE AND ECA MEASUREMENTS

ECE and ECA measurements can provide detailed information on MHD instabilities, electron heat transport, internal electron transport barriers, fast electron dynamics, fast particle-driven modes and high frequency temperature fluctuations. This section reviews some recent ECE and ECA measurements. Significant new results from 2-D ECE imaging of sawtooth reconnections and tearing modes will be discussed in section IV.

Recently, low frequency (8-12 Hz) T_e oscillations have been discovered with ECE radiometry during ECCD discharges on the TCV tokamak [44, 45]. These oscillations appear in two types of plasmas; fully non-inductive discharges with ECCD and discharges with a combination of Ohmic heating and ECCD (Fig. 4). The oscillations look similar to oscillations seen in fully non-inductive LHCD plasmas with reversed central shear in Tore Supra [46]. They have a non-helical structure and interact strongly with existing MHD to significantly perturb the heat and current transport.

On TCV, ECE can be measured simultaneously with radiometers located on the HFS (78-114 GHz) and LFS (65-99 GHz) of the plasma. Measurements with the two ECE radiometers are being used, in conjunction with the 3-D NOTEC code [47], to study ECE spectra from ECCD discharges where up to 50% of the kinetic energy is stored in non-thermal electrons. One such discharge had 1 MW of on-axis ECCD, an electron internal transport barrier, a central electron density of 2×10^{19} m^{-3} and a central electron temperature of 7 keV, measured by Thomson scattering. The ECE spectra from the HFS and LFS radiometers could be simulated by introducing a non-thermal electron population with an energy of 35 keV perpendicular to the magnetic field and an energy

of 1.5 keV parallel to the magnetic field. The non-thermal population density was 20% of the total electron density.

Sawtooth oscillations have been recently studied in the Aditya tokamak in Gandhinagar, India [48] using two 8-channel radiometers operating at 60-90 GHz [49] and 27-39 GHz. The radiometers measure second and third harmonic ECE on Aditya, which has Ohmically-heated plasmas with a major radius of 0.75 m, a minor radius of 0.25 m and a toroidal field of 0.75 T. Heat pulses generated during sawtooth reconnections were observed to exhibit ballistic propagation similar to that measured earlier in the TFTR and DIII-D tokamaks in the USA [50].

Bursts of non-thermal ECE during Quiescent H-mode plasmas in the DIII-D tokamak in San Diego have recently been reported [51]. The bursts coincide with the presence of an edge harmonic oscillation (EHO) [52]. Previously intense (T_{rad} > 10-1000 keV) non-thermal ECE bursts had been reported that were correlated with ELM's in JET [53], TFTR [54] and DIII-D [55], and high β disruptions in TFTR [56]. A prominent feature of the EHO ECE bursting is that there is a threshold MHD amplitude for appearance of the ECE bursts. This is illustrated in Fig. 5 where the bursting turns on as the n=1 EHO mode amplitude exceeds $1x10^{-4}$ T and then turns off when the mode amplitude drops below the same level, while major plasma parameters remain unchanged. For ELM or disruption triggered bursts the emission frequency is downshifted from the ECE resonance frequency corresponding to the location of the ELM or disruption. Surprisingly, the EHO ECE burst appears at an emission frequency that is up-shifted from the ECE resonant frequency corresponding to the location of the EHO.

Fast particle-driven instabilities can seriously degrade the confinement of fusion plasmas. In the Tore Supra tokamak, high frequency (40-200 kHz) Toroidicity-induced Alfvén Eigenmodes (TAE) are triggered during discharges heated with hydrogen minority ion cyclotron range of frequency heating (ICRH) and lower hybrid current drive (LHCD). Barely trapped fast electrons drive low frequency (5-20 kHz) electron fishbone instabilities during LHCD, ECCD and ECRH. Electron temperature fluctuations associated with these modes have been studied [57] with a 78-110 GHz, 32-channel heterodyne ECE radiometer [58]. To measure these low amplitude perturbations, where $\Delta T_e/T_e < 1\%$, a correlation technique [31, 59] was used to overcome the intrinsic thermal noise of the T_e measurement, which was typically $\Delta T_e/T_e \sim 4\%$. The correlation technique used in this case involved integrating the cross-correlation function of two ECE signals emitted from adjacent plasma volumes. Using this technique turbulence levels were determined to be in the 0.1- 0.3 % range in RF-heated Tore Supra plasmas. Fast particle-driven coherent mode amplitudes > 0.3% were measured by correlating ECE signals for 15 ms.

The ECE correlation technique employed on Tore Supra was first used 15 years ago; the technique was developed to measure T_e perturbations that were smaller than the T_e resolution limit set by the intrinsic radiation noise. For a typical heterodyne ECE radiometer, with a receiver bandwidth of 500 kHz and a frequency response of 250 kHz this limit is $\Delta T_e/T_e \sim 2\%$. Correlation analysis can be used to measure fluctuations far below this level. For example, fluctuations associated with TAE modes or modes driven by hot ions. Two correlation schemes have proven successful in practice; correlating ECE in separate frequency bands, the technique used in the experiments on Tore Supra, and correlating ECE signals from two separate radiometers. A current review

summarizing ECE correlation radiometry techniques and recent ECE correlation measurements is presented in this issue of *Fusion Science and Technology* [60].

A 70 GHz 400 kW gyrotron has been used to study single pass electron cyclotron wave absorption oblique to the magnetic field in the Heliotron-J helical-axis device at Kyoto University in Japan [61, 62]. The transmitted wave power was measured and the dependence of the absorption on the plasma electron density, the polarization of the launched power and the electron cyclotron resonance position was investigated. Measurements were compared to a numerical calculation by the TRECE ray tracing code [63] that included a detailed model of the 3-D magnetic field and used a neural network algorithm to reduce the computation time. Both O-mode and X-mode polarized absorption were investigated. The single pass absorption for the summation of the two polarizations agreed well with the numerical calculation at low densities, where refraction was minimal. A polarization scanning experiment, and the TRECE numerical simulation of the experiment, clearly showed the Cotton-Mouton plasma birefringence effect which gives rise to an oscillation in the transmitted wave intensity.

IV. ADVANCES IN 2-D ECE IMAGING

Until the early 1990's ECE T_e measurements employed a single antenna to collect the emission along a viewing chord with a monotonic magnetic field gradient. This arrangement allowed reconstruction of a 1-D T_e profile. In some instances rigid poloidal rotation of the plasma has been used to successfully reconstruct 2-D T_e images from a single antenna, providing valuable information on plasma MHD behavior [64, 65]. But true 2-D ECE T_e imaging requires an antenna array [66]. Figure 6 shows a schematic layout of a 2-D heterodyne ECE imaging diagnostic. An imaging lens focuses ECE onto a vertical array of antennas and Schottky detectors connected to multi-channel or

frequency scanning heterodyne radiometers. A shared local oscillator scans the receive frequency of each radiometer. This arrangement yields $T_e(R,t)$ profiles for each of the horizontal chords, allowing a $T_e(R,Z,t)$ image to be reconstructed (where Z is the vertical direction). High-resolution imaging is achieved by matching the Gaussian beam pattern of the imaging lens to the acceptance angle of the antennas in the array. As in a conventional 1-D ECE T_e diagnostic, horizontal resolution is limited by the rf bandwidth of the radiometers, Doppler and relativistic broadening, and the magnetic field gradient along each viewing chord. Practically, the achievable image resolution is ~ 1 cm in the major radial and poloidal directions. ECE intensity interferometry [60] can be combined with 2-D ECE imaging to image small temperature fluctuations related to broadband turbulence, fast-particle driven Alfvén eigenmodes or MHD instabilities.

The first implementation of a 2-D ECE imaging diagnostic, using a 20-channel 90-120 GHz imaging array, was on the TEXT-U tokamak in the USA [67]. Later a 16-channel 100-140 GHz 2-D ECE imaging system was installed on the RTP tokamak at the FOM Institute for Plasma Physics in the Netherlands [68]. More recently a 2-D ECE imaging system was installed on the LHD stellarator and the GAMMA-10 tandem mirror device in Japan [69, 70], and the RTP 16-channel 2-D ECE imaging diagnostic was moved to the TEXTOR tokamak at Forschungszentrum, Jülich [66, 70-74].

The TEXTOR 2-D, second harmonic, X-mode, ECE imaging diagnostic has recently been used in a detailed study of the sawtooth crash [76-78] and an investigation of NTM suppression by ECRH [74, 79]. Figure 7 shows a schematic of the TEXTOR, 95-130 GHz, 2-D ECE imaging system, which is combined with a microwave imaging reflectometer (MIR) that operates at ~88 GHz. In the TEXTOR ECE imaging diagnostic each of 16 antennas in the array is connected to an 8-channel radiometer, yielding a 128-

element image. The region imaged in the TEXTOR plasma can be moved from the LFS to HFS of the axis. To provide electron temperature profile data, the ECE imaging signals are cross-calibrated to a Thomson scattering system that shares the same viewport.

TEXTOR 2-D ECE imaging data on the HFS of the magnetic axis shown in Fig. 8 clearly shows detailed images of a sawtooth reconnection. Reconnections were found to be highly localized and were observed at many places near the q = 1 rational surface, not just towards the LFS [77]. The combination of kink and local pressure driven instabilities leads to a small poloidally localized puncture in the magnetic surface. The imaging data only partially agree with existing models of sawtooth reconnection [78]. The initial stages of the reconnection look similar to predictions of the ballooning model [80, 81], except that the model predicts only reconnections on the LFS. The intermediate and later stages of the reconnection resemble a full reconnection model [82, 83], although the magnetic island behavior is only partially consistent with that model.

Recently, 2-D ECE imaging measurements have been used to reveal the mechanism by which NTMs are suppressed by ECRH in TEXTOR [74, 79]. Electron cyclotron waves can suppress NTM islands by either driving non-inductive current in the island with ECCD [84] or by heating the island with ECRH [85]. ECCD is thought to be more effective, but in experiments on TEXTOR, ECRH has been shown to be particularly effective at suppressing NTM's. In the TEXTOR experiments 2-D ECE imaging has been used to observe the ECRH suppression mechanism at the q=2 surface on the LFS of the plasma magnetic axis. Results are summarized in Fig. 9. Since the ECE imaging diagnostic covers less than 10% of the circumference of the q=2 surface on the LFS (Fig. 9(a)), the ECE imaging data for one full rotation period is mapped onto a poloidal shell to reconstruct the poloidal mode structure, assuming rigid poloidal rotation of the q=2

surface. Singular value decomposition (SVD) splits the data from the 8x16 image into 128 pairs of space and time eigenvectors. Keeping only the largest eigenvectors from the SVD filters most of the incoherent noise while retaining all physically important data, but without compromising the spatial or temporal resolution. Figure 9 shows a reconstruction of the island during the three main stages of the suppression process. Initially, the island is still 'flat', with very small temperature gradients inside the island (Fig. 9(a)). The hot plasma, deformed by the island, is clearly visible. Figure 9(b) shows the situation about 10 ms after ECRH is turned on, when the temperature inside the island is peaked. Figure 9(c) shows the steady state situation, more than 100 ms after the ECRH is turned on, with the island suppressed to about half its initial size.

V. EBE RESEARCH ON OVERDENSE PLASMAS

Magnetically confined plasma devices that operate in a regime where the electron density is sufficiently high that the electron plasma frequency far exceeds the electron cyclotron frequency ($\omega_{pe} >> \omega_{ce}$) cannot use established ECE or ECA diagnostic techniques. This regime is often referred to as "overdense". Plasma devices that operate in this regime include reversed field pinches, spherical tori, and higher aspect ratio tokamaks and stellarators that operate at high plasma pressures in relation to their confining magnetic fields, that is at high β. The electrostatic electron Bernstein wave (EBW) [86] propagates perpendicular to the magnetic field in the overdense regime and it is strongly emitted and absorbed at EC resonances. The typical optical depth for EBE in overdense plasma is much higher than for ECE in underdense plasma [87]. These characteristics make thermal EBE attractive as a $T_e(R,t)$ diagnostic for overdense plasmas. However there are two challenges in using EBE as a plasma diagnostic; one is that EBWs cannot propagate outside the upper hybrid resonance (UHR) that surrounds

overdense plasma. Consequently, EBE diagnostics rely on mode conversion of the EBWs to electromagnetic waves in the vicinity of the UHR to couple EBE to an antenna outside the plasma. EBE can convert to electromagnetic waves outside the plasma by two coupling schemes; either by tunneling perpendicular to the magnetic field to the X-mode (B-X conversion) [19] or by coupling obliquely to the magnetic field to the O-mode (B-X-O conversion) [20]. The other challenge in using EBE as a diagnostic is that the propagation and dispersion of the EBW is a complicated function of both the local magnetic field and electron temperature. A viable EBE $T_e(R)$ diagnostic therefore usually requires considerable numerical modeling and analysis in order to reconstruct $T_e(R)$.

$T_e(R)$ was first measured successfully with EBE radiometry by using B-X-O conversion on the Wendelstein-7AS stellarator (W7-AS) [21, 22]. Several years later, $T_e(R)$ was measured using B-X conversion on the CDX-U spherical torus [88]. In addition to measuring the electron temperature profile evolution, the 4-12 GHz B-X radiometer on CDX-U measured the electron thermal diffusivity [89] and the magnetic field profile [90]. In the CDX-U experiments, B-X conversion was enhanced to ~100% by using a local limiter to modify the electron density scale length at the UHR in front of the antenna. While this technique is applicable to relatively low temperature spherical torus plasmas, like CDX-U where $T_e \sim$ 10-20 eV at the plasma edge, it is not easily applied to hotter spherical torus devices, like the Mega Amp Spherical Tokamak (MAST) in England or the National Spherical Torus Experiment (NSTX) in the USA.

Extensive EBE studies, via B-X-O conversion, have been conducted on MAST, in the frequency range 16-67 GHz, covering the first 6 EC harmonics [91-94]. There are two EBE heterodyne radiometers on MAST. One radiometer is a 12-channel instrument covering 54-66 GHz with 1 GHz spectral and 10 μs temporal resolution. This radiometer

operates around the frequency of the 1 MW 60 GHz heating system on MAST and shares the heating system's antennas and transmission lines. To maintain the mode purity, the radiometer is connected to one of the TE_{01} transmission lines used for heating via a mode converter. This arrangement provides exactly the same polarization and beam pattern for the EBE measurements as is employed in heating experiments. The other radiometer is a frequency scanning radiometer [95] that covers 16-60 GHz. A typical EBE spectrum from this later radiometer during a high density H-mode is shown in Fig. 10. Fundamental and second harmonic EBE can be clearly seen during the shot. In general, the observed EBE spectral behavior is consistent with the theory of mode coupling and EBW propagation in spherical torus plasmas. However, some features of the EBE spectrum, especially during the H-mode [91, 92], are not fully understood and require further research.

Approximately 80% fundamental B-X-O conversion has been measured during NSTX L-mode plasmas with a 12-18 GHz radiometer [96]. The time evolution of the EBE radiation temperature and its polarization agreed well with a numerical simulation that included 3-D EBW ray tracing and a 1-D full wave mode conversion model [97]. However in NSTX H-mode plasmas measured B-X-O conversion efficiencies were much lower than the level predicted by the numerical simulation [98, 99]. Recently, more detailed measurements, using two remotely steered quad-ridged antennas connected to 8-18 GHz and 18-40 GHz radiometers [100] continue to show almost no EBW coupling from H-mode plasmas.

Measurements of B-X conversion on the Madison Symmetric Torus (MST) reversed field pinch in the USA have yielded intrinsic B-X conversion efficiencies of up to ~ 75% and EBE from MST was confirmed to be predominantly X-mode polarized, as expected.

[101]. On the TST-2 spherical torus in Japan a B-X EBE diagnostic, that combined a hetreodyne EBE radiometer with a reflectometer, measured EBE between 5 and 12 GHz and the density profile in front of the radiometer antenna [102]. B-X mode conversion efficiencies of 50-80% were deduced from a 1-D full-wave calculation and an electron temperature profile was successfully reconstructed from the fundamental and second harmonic EBE.

Recent EBE modeling with the 3-D ray tracing code GENRAY [103] show that energetic electrons, expected during EBW current drive (EBWCD) in NSTX, will generate EBE that dominates the emission from thermal electrons. At $\beta \sim 40\%$, central thermal EBE measurements may not be possible if there are intervening non-thermal electrons driven by EBWCD. Modeling non-thermal EBE behavior is inherently more challenging than modeling non-thermal ECE. For example, the parallel refractive index of EBWs can oscillate about zero as the wave propagates in the plasma, creating a "staircase-like" effect in the EBE frequency spectrum. Interpretation of EBE from non-thermal distributions will clearly require a close interaction between experimental measurements and numerical modeling. EBE research appears to have reached a point in its development that is similar to where ECE research was 25-30 years ago.

VI. CHALLENGES FOR ECE MEASUREMENTS ON ITER

ECE spectra from high temperature reactor-grade plasmas operating at central electron temperatures of 20-40 keV, such as those expected in ITER, will exhibit a large relativistic downshift and broadening [104-106]. These relativistic effects limit the radial resolution of $T_e(R)$ measurements and the ability to measure T_e near the magnetic axis. When ECE is measured perpendicular to the confining magnetic field near the plasma midplane, absorption from the downshifted third harmonic EC resonance makes second

harmonic X-mode measurements of T_e near the axis of ITER impossible for $T_e(0) > 15$ keV. Similarly, O-mode fundamental measurements of central T_e in ITER are only possible up to ~ 30 keV. Furthermore, at $T_e \sim 30$ keV the major radial resolution of O-mode fundamental measurements is degraded to 0.15-0.2 m, and where dT_e/dR is large [106], such as in the vicinity of an internal electron transport barrier or edge H-mode pedestal, resolution is degraded further to 0.2 – 0.3 m. Near-vertical ECE measurements can significantly reduce harmonic overlap, but at high T_e relativistic effects extend the region of anomalous dispersion near the EC resonance layer further out from that layer, bending rays away from the resonance and again preventing T_e measurements near the axis [104].

Recently, it has been proposed that a an ECE measurement oblique to the magnetic field could allow second harmonic, X-mode measurements of a high temperature reactor-grade tokamak plasma up to T_e~24 keV and fundamental, O-mode measurements up to T_e ~50 keV [107]. In the proposed technique the angle between the antenna sightline and the equatorial plane (θ_{port}) is varied to minimize relativistic broadening and hence the frequency overlap between second and third harmonic ECE. The Trubnikov [108] expression for the emissivity perpendicular to the magnetic field has been extended for oblique propagation for plasmas with a relativistic Maxwellian velocity distribution. Calculations for second harmonic X-mode ECE from a plasma with JT-60 tokamak parameters, namely plasma major radius (R_o) = 3.4 m, minor radius (a_p) = 1 m, electron density (n_e) = 2×10^{19} m^{-3}, and axial toroidal magnetic field ($B_T(0)$) = 4T, but with $T_e(0)$ increased to 25 keV, show that it is possible to recover a measurement of $T_e(0)$ by decreasing θ_{port} from 90^o to 60^o (Fig. 11). Similarly, measurements up to

$T_e(0) \sim 50$ keV are predicted for fundamental O-mode ECE. However, when n_e, $B_T(0)$ or a_p/R_o increase, the maximum measurable $T_e(0)$ decreases.

EC radiation will be a major player in plasma energy transport in ITER [109]. For some ITER steady-state scenarios, where $T_e(0) > 35$ keV, power loss due to ECE is expected to exceed the loss due to bremsstrahlung and EC radiation transport will be comparable to, or even exceed, the plasma energy transport. In ITER plasmas changes in wall reflectivity are expected to play a major role when wall reflectivity is > 60%. For example, increasing wall reflectivity from 60 to 100% could increase $T_e(0)$ by ~ 30%. Also a relatively small population of fast electrons with energies above the bulk of the electron thermal distribution can modify and enhance the EC power loss [110]. Consequently, on ITER it will be important to measure the total ECE loss with broadband, wide angle antennas and EC radiation transport will need to be explicitly included in the plasma transport analysis. Clearly ECE measurements will be even more important on ITER than they are on present-day devices.

In optically thick magnetically-confined tokamak plasmas where $T_e \leq 7$ keV, $T_e(R)$ measured by ECE is generally in good agreement with $T_e(R)$ measured by laser Thomson scattering (TS), with any differences being less than 10%. However, there has been growing evidence that this may not be true at higher electron temperatures, at least under some conditions. Discrepancies between ECE and TS T_e measurements in plasmas with $T_e > 7$ keV were first reported in the Tokamak Fusion Test Reactor (TFTR) in the USA [111, 112]. The discrepancy between ECE and TS was reported to increase with increasing T_e. More recently, a similar discrepancy was reported in the JET tokamak [113]. An analysis of the JET ECE data suggests that there may be non-Maxwellian distortions in the bulk electron velocity distribution at around 1.5 times the average

thermal momentum in regions of the plasma where $T_e \geq 7$ keV. Similar effects have been reported during ECRH plasmas in the FTU tokamak in Italy [114]. It is clear that understanding the discrepancy between ECE and TS T_e measurements at high T_e is important for ITER and other future reactor-grade nuclear fusion devices. An obliquely-viewing ECE diagnostic has been installed on JET to simultaneously measure the ECE at ~0^o, ~10^o and ~20^o with respect to the normal to the magnetic field, in order to study the behavior of the bulk electron distribution at high T_e with good spatial and energy resolution [33-35]. A similar oblique ECE view is being considered for the proposed ITER midplane ECE diagnostic [106]. It may also be possible to use the back scattering antenna array on the receiver side of the proposed ITER microwave fast ion collective Thomson scattering diagnostic [115] for oblique ECE measurements.

VII. SUMMARY

Over the quarter-century since it was first successfully used to measure the $T_e(R)$ profile, ECE has evolved into an invaluable tool for studying the physics of magnetically confined plasma in nuclear fusion research devices. There have been significant recent developments in ECE research and ECE-related technology. 2-D ECE imaging and intensity correlation techniques are providing a deeper understanding of MHD behavior and the role of electron collective turbulence in electron thermal transport. Real-time ECE analysis is enabling dynamic NTM suppression by ECCD and ECRH. EBE research is opening the possibility of extending ECE diagnostic techniques to the study of "overdense" high β plasmas. As the electron temperature of fusion research devices has increased, relativistic effects have become increasingly important in the analysis of ECE measurements. There are hints of non-Maxwelian behavior in the bulk electron distribution at $T_e > 10$ keV that has potential significance for ITER. For the first time

ITER presents us with a truly reactor-grade plasma, it also presents significant challenges for ECE measurements in the next quarter-century.

ACKNOWLEDGEMENTS

This work was supported by US Department of Energy contract no. DE-AC02-76CH03073. The author thanks participants at the EC-14 workshop for providing copies of their papers and presentations at the workshop and for copies of their recent publications.

REFERENCES

1. I. H. HUTCHINSON, *Principles of Plasma Diagnostics*, 2nd Edition (Cambridge University Press, New York, 2002) pp. 155-210.

2. A. E. COSTLEY, et. al., "Electron Cyclotron Emission from a Tokamak Plasma: Experiment and Theory", *Phys. Rev. Lett*. **33**, 758 (1974).

3. F. ENGELMANN and M. CURATOLO, "Cyclotron Radiation from a Rarefied Magnetoplasma", *Nucl. Fusion* **13**, 497 (1973).

4. C.M. CELATA and D.A. BOYD, "Cyclotron Radiation as a Diagnostic Tool for Tokamak Plasmas.", *Nucl. Fusion* **17**, 735 (1977).

5. I. H. HUTCHINSON and D. S. KOMM, "Electron Cyclotron Emission in Alcator Tokamak", *Nucl. Fusion* **17**, 1077 (1977).

6. W.H.M. CLARK, "Precision of Electron Cyclotron Emission Measurements from DITE Tokamak", *Plasma Phys.* **25**, 1501 (1983).

7. J. HOSEA, et al., "Electron Cyclotron Emission from the Princeton Large Tokamak", *Phys. Rev. Lett*. **39**, 408 (1977).

8. P.C. EFTHIMION, et al., "Ordinary-Mode Fundamental Electron-Cyclotron Resonance Absorption and Emission in the Princeton Large Torus" *Phys. Rev. Lett.* **44**, 396 (1980).

9. M. BORNATICI, et. al., "Electron Cyclotron Emission and Absorption in Fusion Plasmas", *Nucl. Fusion* **23**, 1153 (1983).

10. I. FIDONE and G. GIRUZZI, " Diagnostics of Superthermal Electrons using Cyclotron Radiation",*Nucl. Fusion* **30**, 803 (1990).

11. M. BORNATICI and F. ENGELMANN, "Electron-Cyclotron Absorption and Emission: 'Vexatae quaestiones' ", *Phys. Plasmas* **1**, 189 (1994).

12. Y. NAGAYAMA, et al., "Observation of Ballooning Modes in High-Temperature Tokamak Plasmas", *Phys. Rev. Lett*. **69**, 2376 (1992).
13. Z. CHANG, et al., "Off-Axis Sawteeth and Double-Tearing Reconnection in Reversed Magnetic Shear Plasmas in TFTR", *Phys. Rev. Lett*. **77**, 3553 (1996).
14. G. CIMA, et al., "Core Temperature Fluctuations and Related Heat Transport in the Texas Experimental Tokamak-Upgrade", *Phys. Plasmas* **2**, 720 (1995).
15. T.C. LUCE, P.C. EFTHIMION and N. FISCH, "Superthermal Electron Distribution Measurements from Polarized Electron Cyclotron Emission", *Rev. Sci. Instrum.* **59**, 1593 (1988).
16. S. PREISCHE, P.C. EFTHIMION and S. KAYE, "Radially Localized Measurements of Superthermal Electrons using Oblique Electron Cyclotron Emission", *Phys. Plasmas* **3**, 4065 (1996).
17. J.F.M. VAN GELDER, et al., "The Electron Cyclotron Absorption Diagnostic at the Rijnhuizen Tokamak Project", *Rev. Sci. Instrum*. **68**, 4439 (1997).
18. D.A. BOYD et al., "A System to Measure Suprathermal Electron Distribution Functions in Toroidal Plasmas by Electron Cyclotron Wave Absorption", *Rev. Sci. Instrum*. **68**, 496 (1997).
19. A.K. RAM, and S.D. SCHULTZ, "Excitation, Propagation, and Damping of Electron Bernstein Waves in Tokamaks" *Phys. Plasmas* **7**, 4084 (2000).
20. J. PREINHAELTER and V. KOPÉCKY, "Penetration of High-Frequency Waves into a Weakly Inhomogeneous Magnetized Plasma at Oblique Incidence and their Transformation to Bernstein Modes", *J. Plasma Phys.* **10**, 1 (1973).

21. H.P. LAQUA, H.J. HARTFUSS AND W7-AS TEAM, "Electron Bernstein Wave Emission from an Overdense Plasma at the W7-AS Stellarator", *Phys. Rev. Lett*. **81**, 2060 (1998).

22. F. VOLPE, and H.P. LAQUA, "BXO Mode-Converted Electron Bernstein Emission Diagnostic", *Rev. Sci. Instrum*. **74**, 1409 (2003).

23. D.H. MARTIN and E. PUPLETT, "Polarized Interferometric Spectroscopy for the Millimeter and Submillimeter Spectrum", *Infrared Phys.* **10**, 105 (1970).

24. A.E. COSTLEY, et al., "First Measurements of ECE from JET" *Proceedings of the 4th Workshop on ECE and ECRH* (Rome, Italy, 1984) (Serie Simposi of ENEA) p.1.

25. F. STAUFFER, et al., "Broadband Measurement of Electron Cyclotron Emission in TFTR using a Quasioptical Light Collection System and a Polarizing Michelson Interferometer", *Rev. Sci. Instrum*. **59**, 2139 (1988).

26. A. CAVALLO and R. CUTLER, "Absolute Calibration of a Ten-Channel Grating Polychromator for Electron Temperature Measurements on Princeton Large Torus", *Rev. Sci. Instrum*. **56**, 931 (1985).

27. A. EBERHAGEN, "A Very Rapidly Scanning Monochromator with Low Internal Losses but High Spectral Resolution and Repetition Rate for Millimetre and Submillimetre Wavelengths and Below", *Infrared Phys.* **19**, 389 (1979).

28. P.C. EFTHIMION, et al., "A Fast-Scanning Heterodyne Receiver for Measurement of the Electron Cyclotron Emission from High-Temperature Plasmas", *Rev. Sci. Instrum*. **50**, 949 (1979).

29. G. TAYLOR, et al., "Fast Scanning Heterodyne Receiver for the Measurement of the Time Evolution of the Electron Temperature Profile on the Tokamak Fusion Test Reactor", *Rev. Sci. Instrum*. **55**, 1739 (1984).

30. H. J. HARTFUSS and M. TUTTER, “Fast Multichannel Heterodyne Radiometer for Electron Cyclotron Emission Measurement on Stellarator W VII-A”, *Rev. Sci. Instrum*. **56**, 1703 (1985).

31. SATTLER and HARTFUSS, “Intensity Interferometry for Measurement of Electron Temperature Fluctuations in Fusion Plasmas”, *Plasma Phys. Control. Fusion* **35**, 1285 (1993).

32. H. J. HARTFUSS, et al., “Heterodyne Methods in Millimetre Wave Plasma Diagnostics with Applications to ECE, Interferometry and Reflectometry”, *Plasma Phys. Control. Fusion* **39**, 1693 (1997).

33. P. BURATTI and M. ZERBINI, “A Fourier Transform Spectrometer with Fast Scanning Capability for Tokamak Plasma Diagnostic”, *Rev. Sci. Instrum*. **66**, 4208 (1995).

34. C. SOZZI, et al, “The Multichannel Extension of the Martin-Puplett Interferometer for Perpendicular and Oblique ECE Measurements on JET”, *Proc. 14th Joint Workshop on ECE and ECRH*, (Santorini, Greece, May 2006) ed. Avrilios Lazaros (Heliotopos Conferences Ltd., Athens, Greece, 2006, ISBN: 960-89228-2-8) p. 157.

35. A.SIMONETTO, et al., **“**Conceptual Design of The Optical Scheme for a Multichannel Martin Puplett Interferometer for Perpendicular and Oblique ECE Measurements On JET”, *Proc. 14th Joint Workshop on ECE and ECRH*, (Santorini, Greece, May 2006) ed. Avrilios Lazaros (Heliotopos Conferences Ltd., Athens, Greece, 2006, ISBN: 960-89228-2-8) p. 238.

36. C. SOZZI, et al., “Optical Design of the Oblique ECE Antenna System for JET “, *Fusion Eng. Des.* **74**, 691 (2005).

37. J.L SÉGUI, et al. “Real Time ECE Electron Temperature Profile Measurements on the Tore-Supra Tokamak”, *Proc. 14th Joint Workshop on ECE and ECRH*, (Santorini, Greece, May 2006) ed. Avrilios Lazaros (Heliotopos Conferences Ltd., Athens, Greece, 2006, ISBN: 960-89228-2-8) p. 199.

38. J.W. OOSTERBEEK, et al. “Design of a Dedicated ECE Diagnostic for Feedback Control of Instabilities by ECRH”, *Proc. 14th Joint Workshop on ECE and ECRH*, (Santorini, Greece, May 2006) ed. Avrilios Lazaros (Heliotopos Conferences Ltd., Athens, Greece, 2006, ISBN: 960-89228-2-8) p. 232.

39. T.P. GOODMAN, et al., **“**First Measurements of Oblique ECE with a Real-Time Moveable Line-of-Sight on TCV”, *Proc. 14th Joint Workshop on ECE and ECRH*, (Santorini, Greece, May 2006) ed. Avrilios Lazaros (Heliotopos Conferences Ltd., Athens, Greece, 2006, ISBN: 960-89228-2-8) p. 188.

40. O.TUDISCO, et al., “Oblique ECE Measurements on FTU”**,** *Proc. 14th Joint Workshop on ECE and ECRH*, (Santorini, Greece, May 2006) ed. Avrilios Lazaros (Heliotopos Conferences Ltd., Athens, Greece, 2006, ISBN: 960-89228-2-8) p. 222.

41. R. CAVAZZANA and M. MORESCO, “Multilayer vacuum window for wide-band microwave plasma diagnostic systems” *Rev. Sci. Instrum*. **77** 10E921 (2006).

42. A. DINKLAGE, et al., “Topics and Methods for Data Validation by Means of Bayesian Probability Theory”, *Fusion Sci. Technol*., **46**, 355 (2004).

43. N.B. MARUSHCHENKO, et al, "Optimization of ECE Diagnostic for W7-X Stellarator", *Proc. 14th Joint Workshop on ECE and ECRH*, (Santorini, Greece, May 2006) ed. Avrilios Lazaros (Heliotopos Conferences Ltd., Athens, Greece, 2006, ISBN: 960-89228-2-8) p. 216.

44. V.S. UDINTSEV et al, "Progress in ECE Diagnostics Development on TCV", *Proc. 14th Joint Workshop on ECE and ECRH*, (Santorini, Greece, May 2006) ed. Avrilios Lazaros (Heliotopos Conferences Ltd., Athens, Greece, 2006, ISBN: 960-89228-2-8) p. 167.

45. V.S. UDINTSEV et al, "Overview of Recent Results of ECE on TCV", submitted to *Fusion Sci. Technol.* (2006).

46. G. GIRUZZI et al., "New Tokamak Plasma Regime with Stationary Temperature Oscillations", Phys. Rev. Lett. **91**, 135001 (2003).

47. R.M.J. SILLEN, "NOTEC, A Code to Simulate Electron Cyclotron Emission Spectra of Plasmas which Include Non-Thermal Populations", Rijnhuizen Report 86-165 (1986).

48. H. K. B. PANDYA, et al., "Study of Sawtooth Oscillations on Aditya tokamak by Electron Cyclotron Emission Measurements", *Proc. 14th Joint Workshop on ECE and ECRH*, (Santorini, Greece, May 2006) ed. Avrilios Lazaros (Heliotopos Conferences Ltd., Athens, Greece, 2006, ISBN: 960-89228-2-8) p. 173.

49. N. CHAUBE and K.K. JAIN, "Superheterodyne Radiometer to Measure Electron Temperature Profile in Aditya Tokamak", *Fusion Eng. Des.* **34-35**, 473 (1997).

50. E.D. FREDRICKSON, et al., "Heat Pulse Propagation Studies on DIII-D and the Tokamak Fusion Test Reactor", *Phys. Plasmas* **7**, 5051 (2000).

51. M.E. AUSTIN, et al., "Investigation of Narrowband ECE Bursts in DIII-D Plasmas", *Proc. 14th Joint Workshop on ECE and ECRH*, (Santorini, Greece, May 2006) ed. Avrilios Lazaros (Heliotopos Conferences Ltd., Athens, Greece, 2006, ISBN: 960-89228-2-8) p. 179.

52. K.H. BURRELL, et al., "Quiescent Double Barrier High-Confinement Mode Plasmas in the DIII-D Tokamak", *Phys. Plasmas* **8**, 2153 (2001).

53. L. PORTE, et al, "First Results with the Upgraded ECE Heterodyne Radiometer on JET", *Proc. 18th European Conf. on Controlled Fusion and Plasma Physics*, (Berlin, Germany, 1991), Vol 15C, Part IV (European Physical Society) p.357.

54. G. TAYLOR, et al., "Intense Electron Cyclotron Emission Bursts during High Power Neutral Beam Heating on TFTR", *Nucl. Fusion* **32**, 1867 (1992).

55. CH. FUCHS and M.E. AUSTIN, "Measurements of Edge-Localized-Mode Induced Electron Cyclotron Emission Bursts in DIII-D", *Phys. Plasmas* **8**, 1594 (2001).

56. A. JANOS, et al., "Bursts of Electron cyclotron emission during ELMs and high β disruptions in TFTR", *Plasma Phys. Control. Fusion* **38**, 1373 (1996).

57. M. GONICHE, et al., "Identification of fast particle triggered modes by means of correlation ECE on Tore Supra", submitted to *Fusion Sci. Technol.* (2006).

58. J.L SÉGUI, et al., "An Upgraded 32-Channel Heterodyne Electron Cyclotron Emission Radiometer on Tore Supra", *Rev. Sci. Instrum.* **76**, 123501 (2005).

59. C. CIMA, et al., "Correlation Radiometry of Electron Cyclotron Radiation in TEXT-U", *Rev. Sci. Instrum.* **66**, 798 (1995).

60. C. WATTS, "A Review of ECE Correlation Radiometry Techniques for Detection of Core Electron Temperature Fluctuations", submitted to *Fusion Sci. Technol.* (2006).

61. K. NAGASAKI, et al., "Measurement of Absorption and Scattering of High Power EC Waves in Heliotron J ", *Proc. 32nd EPS Conf. on Plasma Phys.* (Tarragona, Spain, June 2005), ECA Vol 29C, P-4.104 (2005)

62. K. NAGASAKI, et al., "Measurement of Single Pass EC Absorption Using Transmitted Waves in Heliotron J ", *Proc. 14th Joint Workshop on ECE and ECRH*, (Santorini, Greece, May 2006) ed. Avrilios Lazaros (Heliotopos Conferences Ltd., Athens, Greece, 2006, ISBN: 960-89228-2-8) p. 162.

63. V. TRIBALDOS, et al., "Electron Cyclotron Heating and Current Drive in the TJ-II Stellarator", *Plasma Phys. Control. Fusion* **40**, 2113 (1998).

64. Y. NAGAYAMA, et al., "Tomography of Full Sawtooth Crashes on the Tokamak Fusion Test Reactor", *Phys. Plasmas* **3**, 1647 (1996).

65. Y. NAGAYAMA, et al., "Tomography of (2, 1) and (3, 2) Magnetic Island Structures on Tokamak Fusion Test Reactor", *Phys. Plasmas* **3**, 2631 (1996).

66. H.K. PARK, et al*.,* "Recent Advancements in Microwave Imaging Plasma Diagnostics"*, Rev. Sci. Instrum*. **74,** 4239 (2003).

67. R.P. HSIA, et al*.,* "Hybrid Electron Cyclotron Emission Imaging Array System for Texas Experimental Tokamak Upgrade"*, Rev. Sci. Instrum*. **68,** 488 (1997).

68. B.H. DENG, et al., "Electron Cyclotron Emission Imaging Diagnostic System for Rijnhuizen Tokamak Project", *Rev. Sci. Instrum*. **70**, 998 (1999).

69. A. MASE, et al.," ECE-Imaging Work on GAMMA 10 and LHD", *Fusion Eng. Des.* **53**, 87 (2001).

70. A. MASE, et al., "Application of Millimeter-Wave Imaging System to LHD", *Rev. Sci. Instrum.* **72**, 375 (2001).

71. B.H. DENG, et al., "Electron Cyclotron Emission Imaging Diagnostic on TEXTOR", *Rev. Sci. Instrum*. **72**, 368 (2001).

72. H.K. PARK, et al., "Simultaneous Microwave Imaging System for Density and Temperature Fluctuation Measurements on TEXTOR", *Rev. Sci. Instrum.* **75**, 3787 (2004).

73. G.W. SPAKMAN, et al., "High-Resolution 2D Electron Temperature Measurements via ECE-Imaging", *Proc. 14th Joint Workshop on ECE and ECRH*, (Santorini, Greece, May 2006) ed. Avrilios Lazaros (Heliotopos Conferences Ltd., Athens, Greece, 2006, ISBN: 960-89228-2-8) p. 211.

74. I.G.J. CLASSEN, et al., "2-D ECE temperature measurements inside tearing modes, revealing the suppression mechanism by ECRH at TEXTOR.", *Proc. 14th Joint Workshop on ECE and ECRH*, (Santorini, Greece, May 2006) ed. Avrilios Lazaros (Heliotopos Conferences Ltd., Athens, Greece, 2006, ISBN: 960-89228-2-8) p. 134.

75. C.W. DOMIER, et al., "Upgrades to the TEXTOR Electron Cyclotron Emission Imaging Diagnostic", *Rev. Sci. Instrum*. **77**, 10E924 (2006).

76. H.K. PARK, et al., "Self-Organized T_e Redistribution during Driven Reconnection Processes in High-Temperature Plasmas", *Phys. Plasmas* **13**, 055907 (2006).

77. H.K. PARK, et al., "Observation of High-Field-Side Crash and Heat Transfer during Sawtooth Oscillation in Magnetically Confined Plasmas", *Phys. Rev. Lett.* **96**, 195003 (2006).

78. H.K. PARK, et al., "Comparison Study of 2D Images of Temperature Fluctuations during Sawtooth Oscillation with Theoretical Models", *Phys. Rev. Lett.* **96**, 195004 (2006).

79. I.G.J. CLASSEN, et al., "The Effect of Heating on the Suppression of Tearing Modes in Tokamaks", submitted to *Phys. Rev. Lett.* (2006).

80. W. PARK, et al., "High-β Disruption in Tokamaks", *Phys. Rev. Lett.* **75**, 1763 (1995).

81. Y. NISHIMURA, et al., "Onset of High-n Ballooning Modes during Tokamak Sawtooth Crashes", *Phys. Plasmas* **6**, 4685 (1999).

82. B.B. KADOMTSEV, "Disruptive Instability in Tokamaks", *Sov. J. Plasma Phys*. **1**, 389 (1975).

83. A. SYKES and J.A. WESSON, "Relaxation Instability in Tokamaks", *Phys. Rev. Lett.* **37**, 140 (1976).

84. R.J. LAHAYE, "Neoclassical Tearing Modes and their Control", *Phys. Plasmas* **13**, 055501 (2006).

85. D.A. KISLOV, et al., "The m=2, n=1 Mode Suppression by ECRH on the T-10 Tokamak", *Nucl. Fusion* **37**, 339 (1997).

86. I.B. BERNSTEIN, "Waves in a Plasma in a Magnetic Field", *Phys. Rev*. **109**, 10 (1958).

87. P.C. EFTHIMION, et al., "New Electron Cyclotron Emission Diagnostic for Measurement of Temperature Based Upon the Electron Bernstein Wave", *Rev. Sci. Instrum.* **70**, 1018 (1999).

88. B. JONES, et al., "Controlled Optimization of Mode Conversion from Electron Bernstein Waves to Extraordinary Mode in Magnetized Plasma", *Phys. Rev. Lett.* **90**, 165001 (2003).

89. T. MUNSAT, et al., "Transient Transport Experiments in the Current-Drive Experiment Upgrade Spherical Torus", *Phys. Plasmas* **9**, 480 (2002).

90. B. JONES, et al., "Measurement of the Magnetic Field in a Spherical Torus Plasma via Electron Bernstein Wave Emission Harmonic Overlap", *Phys. Plasmas* **11**, 1028 (2004).

91. V. SHEVCHENKO, et al, "Prospects of EBW Emission Diagnostics and EBW Heating in Spherical Tokamaks", *Proc. 13th Joint Workshop on ECE and ECRH*, (Nizhny Novgorod, Russia, 2004), p. 162.

92. V. SHEVCHENKO, et al, "Electron Bernstein Wave Studies on COMPASS-D and MAST", *Proc. 15th Topical Conference on RF Power in Plasmas,* (Moran, Wyoming, USA, 2003) ed. C. Forest, *AIP Proceedings* **694**, 359 (2003).

93. J. PREINHAELTER, et al., "Influence of Antenna Aiming on ECE in MAST", Rev. Sci. Instrum. **75**, 3804 (2004).

94. V. SHEVCHENKO, et al., "Development of Electron Bernstein Wave Research in MAST", submitted to *Fusion Sci. Technol.* (2006).

95. V. SHEVCHENKO, et al., "ECE Measurements via B-X-O Mode Conversion - a Proposal to Diagnose the q Profile in Spherical Tokamaks", *Proc. 27th EPS Conf. on Control. Fusion and Plasma Phys.* (Budapest, Hungary, June 2000) ECA vol. **25B**, P3.120 (2000).

96. G. TAYLOR, et al., "Efficient Coupling of Thermal Electron Bernstein Waves to the Ordinary Electromagnetic Mode on the National Spherical Torus Experiment", *Phys. Plasmas* **12**, 052511 (2005).

97. J. PREINHAELTER, et al., "EBW simulation for MAST and NSTX experiments", *Proc. of the 16th Topical Conference on RF Power in Plasmas*, (Park City, Utah, USA, 2005) ed. S. Wukitch and P. Bonoli, AIP Proceedings **787**, 349 (2005).

98. G. TAYLOR, et al., "EBW Research on Overdense Plasmas in NSTX", *Proc. 14th Joint Workshop on ECE and ECRH*, (Santorini, Greece, May 2006) ed. Avrilios Lazaros (Heliotopos Conferences Ltd., Athens, Greece, 2006, ISBN: 960-89228-2-8) p. 145.

99. J. URBAN, et al., "EBW Emission Simulations and Plasma Diagnostics", *Proc. 14th Joint Workshop on ECE and ECRH*, (Santorini, Greece, May 2006) ed. Avrilios Lazaros (Heliotopos Conferences Ltd., Athens, Greece, 2006, ISBN: 960-89228-2-8) p. 194.

100. S.J. DIEM, et al., "T_e(R,t) Measurements using Electron Bernstein Wave Thermal Emission on NSTX", *Rev. Sci. Instrum*. **77**, 10E919 (2006).

101. P.K. CHATTOPADHYAY, et al., "Electron Bernstein Wave Emission from an Overdense Reversed Field Pinch Plasma", *Phys. Plasmas* **9**, 752 (2002).

102. S. SHIRAIWA, et al., "Electron Bernstein Wave Emission Diagnostic Assisted by Reflectometry on TST-2 Spherical Tokamak" *Rev. Sci. Instrum*. **74**, 1453 (2003).

103. R.W. HARVEY, et al., "Electron Bernstein Emission Due to Nonthermal Distributions in NSTX", *Proc. 14th Joint Workshop on ECE and ECRH*, (Santorini, Greece, May 2006) ed. Avrilios Lazaros (Heliotopos Conferences Ltd., Athens, Greece, 2006, ISBN: 960-89228-2-8) p. 151.

104. D.V. BARTLETT, "Physics Issues of ECE and ECA for ITER", in *Diagnostics for Experimental Thermonuclear Fusion Reactors*, ed. P.E. Stott et al. (Plenum Press, New York, 1996), p. 183.

105. D.V. BARTLETT and H. BINDSLEV, "Physics Aspects of ECE T_e Measurements in ITER", in *Diagnostics for Experimental Thermonuclear Fusion Reactors 2*, ed. P.E. Stott et al. (Plenum Press, New York, 1998), p. 171.

106. G. VAYAKIS, et al, "ECE Diagnostics for RTO/RC ITER", *Fusion Eng. Des.* **53**, 221 (2001).

107. M. SATO and A. ISAYAMA, "Evaluation of Extended Trubnikov's Emissivity to the Oblique Propagation and Application to Electron Temperature Measurement in a Reactor Grade Tokamak", *Proc. 14th Joint Workshop on ECE and ECRH*, (Santorini, Greece, May 2006) ed. Avrilios Lazaros (Heliotopos Conferences Ltd., Athens, Greece, 2006, ISBN: 960-89228-2-8) p. 205. Also submitted to *Fusion Sci. Technol.* (2006)

108. B.A. TRUBNIKOV, "Magnetic Emission of High Temperature Plasma", Thesis, Institute of Atomic Energy, Moscow, Russia, 1958.

109. F. ALBAJAR, et al., "Importance of Electron Cyclotron Wave Energy Transport in ITER", *Nucl. Fusion,* **45**, 642 (2005).

110. K.V. CHEREPANOV and A.B. KUKUSHKIN, "Influence of Suprathermal Electrons Kinetics on Cyclotron Radiation Transport in Hot Toroidal Plasmas", *Proc. 20th Int. Conf. on Fusion Energy* (Vilamoura, Spain, 2004) (Vienna, IAEA) paper TH/P6-56.

111. G. TAYLOR, et al., "Analysis of Electron Cyclotron Emission Spectra of High Electron Temperature, Supershot Plasmas in TFTR" *Proc. 8th Joint Workshop on ECE and ECRH* (Gut Ising, Germany, 1992) ed. H. HARTFUSS, p. 277.

112. G. TAYLOR, et al., "Electron Cyclotron Emission Measurements on High β TFTR Plasmas", *Proc. 9th Joint Workshop on ECE and ECRH* (Borrego Springs, USA, 1995) ed. J. LOHR (World Scientific, Singapore, 1995), p. 485.

113. E. DE LA LUNA, et al., "Impact of Bulk Non-Maxwellian Electrons on Electron Temperature Measurements", *Rev. Sci. Instrum,* **74**, 1414 (2003).

114. V. KRIVENSKI, et al., "Electron Cyclotron Emission by Non-Maxwellian Bulk Distribution Functions", *Fusion Eng. Des.* **53**, 23 (2001).

115. E. TSAKADZE, et al., "Fast Ion Collective Thomson Scattering Diagnostic for ITER", submitted to *Fusion Sci. Technol.* (2006).

FIGURE CAPTIONS

Figure 1

JET oblique ECE antenna. Photograph reproduced by courtesy of Thomas Keating Ltd. [Reprinted from Fusion Eng. Des. **74**, 691 (2005), C. SOZZI, et al., "Optical Design of the Oblique ECE Antenna System for JET", Copyright 2005, with permission from Elsevier]

Figure 2

Schematic layout Martin-Puplett interferometer with rotating helicoidal mirror.

Figure 3

(a) Schematic layout of TEXTOR "Line of Sight" NTM ECE feedback system and (b) schematic of receiver optics for the ECE feedback system. [Reprinted with permission from J.W. OOSTERBEEK, et al. "Design of a Dedicated ECE Diagnostic for Feedback Control of Instabilities by ECRH", *Proc. 14th Joint Workshop on ECE and ECRH*, (Santorini, Greece, May 2006) ed. Avrilios Lazaros (Heliotopos Conferences Ltd., Athens, Greece, 2006, ISBN: 960-89228-2-8) p. 232.]

Figure 4

Development of temperature oscillation in TCV during a predominantly Ohmically-heated discharge with counter-ECCD on axis in discharge 32035. [Reprinted with permission from V.S. UDINTSEV et al, "Overview of Recent Results of ECE on TCV", submitted to *Fusion Sci. Technol.* (2006).]

Figure 5

Time histories of beam power, MHD mode amplitude, and ECE radiation temperature for a DIII-D discharge with an EHO ECE burst in channels 9 and 10 (the burst saturates the amplifier on channel 9) [Reprinted with permission from M.E. AUSTIN, et al., "Investigation of Narrowband ECE Bursts in DIII-D Plasmas", *Proc. 14th Joint Workshop on ECE and ECRH*, (Santorini, Greece, May 2006) ed. Avrilios Lazaros (Heliotopos Conferences Ltd., Athens, Greece, 2006, ISBN: 960-89228-2-8) p. 179]

Figure 6

Schematic layout of a 2-D ECE imaging system [Reprinted with permission from H. PARK, et al., "Simultaneous Microwave Imaging System for Density and Temperature Fluctuation Measurements on TEXTOR", *Review of Scientific Instruments*, **75**, 3787 (2004). Copyright 2004, American Institute of Physics].

Figure 7

The detailed schematic of the TEXTOR 2-D ECE imaging (ECEI) and microwave imaging reflectometer (MIR) systems: (a) poloidal focusing mirror; (b) toroidal focusing mirror; (c) beam splitter for MIR and ECEI signals; (d) H-plane focusing lens for ECEI system; (e) E-plane focusing lens for ECEI system; (f) flat mirror; and (g) moveable lens for the ECEI system focal depth change (*h*) beam splitter (50/50) for MIR source beam and signal (*i* and *j*) MIR source beam and collimating lens, (k) MIR detection array, (*m*) ECEI detection array. [Reprinted with permission from H. PARK, et al, "Simultaneous Microwave Imaging System for Density and Temperature Fluctuation Measurements on TEXTOR", *Review of Scientific Instruments*, **75**, 3787 (2004). Copyright 2004, American Institute of Physics.]

Figure 8

2-D images of a sawtooth crash at the HFS of TEXTOR are shown with the time history of the electron temperature fluctuation at Z = 0, R = 148 cm. The reconnection process is similar to that observed at the low field side. A sharp temperature point develops with the moderate swelling of the hot core (frame 4) but fails to lead to reconnection on the first attempt. In the second attempt, the sharp temperature point accompanied with the strong swelling of the hot spot (kink instability) (frames 6 and 7) succeeds in crossing the inversion radius through a small opening (~ a few cm). The opening increases up to ~10 cm, and the heat flows out from the hot spot. The nested magnetic surfaces from the core push the heat flow out (frame 11), and, eventually, symmetry is recovered (frame 12). [Reprinted with permission from H. K. PARK, et al., "Observation of High-Field-Side Crash and Heat Transfer during Sawtooth Oscillation in Magnetically Confined Plasmas", *Physical Review Letters* **96**, 195003 (2006). Copyright 2006]

Figure 9

Poloidal reconstruction of a magnetic island during suppression by ECRH on TEXTOR measured by 2-D ECE imaging. Representation of the island mode structure from 2-D ECE measurements on the LFS reconstructed during a full rotation period of 2 ms. (a) flat island, (b) heated island, 10 ms after ECRH is turned on, and c) suppressed island, more than 100 ms after ECRH is turned on. [Reprinted with permission from I.G.J. CLASSEN, et al., "2-D ECE Temperature Mmeasurements Inside Tearing Modes, Revealing the Suppression Mechanism by ECRH at TEXTOR", *Proc. 14th Joint Workshop on ECE and ECRH*, (Santorini, Greece, May 2006) ed. Avrilios Lazaros (Heliotopos Conferences Ltd., Athens, Greece, 2006, ISBN: 960-89228-2-8) p. 134.]

Figure 10

EBE spectrum measured during MAST plasma shot #7798. Red areas correspond to high EBE intensity. 60 GHz microwave power was injected at 0.21-0.24 s. The time dependence of the plasma current (I_p) , radius of the last closed flux surface (R_{LCFS}) and the toroidal field current (I_{TF}) is also plotted. [Reprinted with permission from V. SHEVCHENKO, et al., "Development of Electron Bernstein Wave Research in MAST" submitted to *Fusion Sci. Technol.* (2006).]

Figure 11

Measured $T_e(r/a)$ for cases with different θ_{port}. Dotted line represents electron temperature measured by second and third harmonic X-mode ECE. [Reprinted with permission from M. SATO and A. ISAYAMA, "Evaluation of ECE Spectra on the Oblique Propagation and Application to Electron Temperature Measurement in a Reactor Grade Tokamak", submitted to *Fusion Sci. Technol.* (2006).]

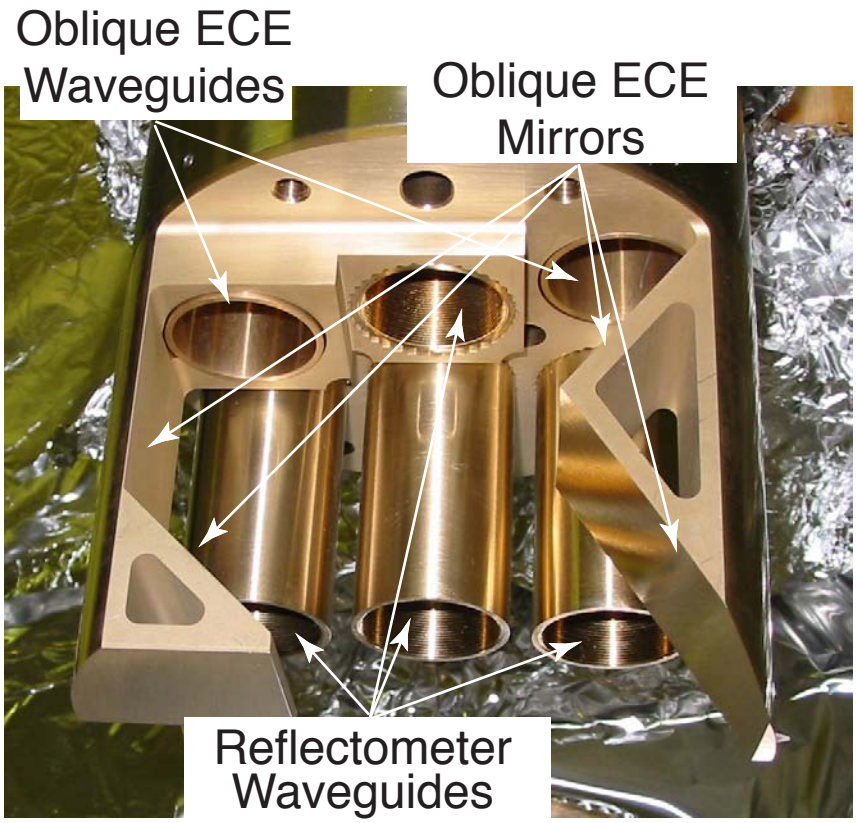

Recent Developments in Electron Cyclotron Emission Research on Magnetically Confined Plasmas / Gary Taylor / Figure 1

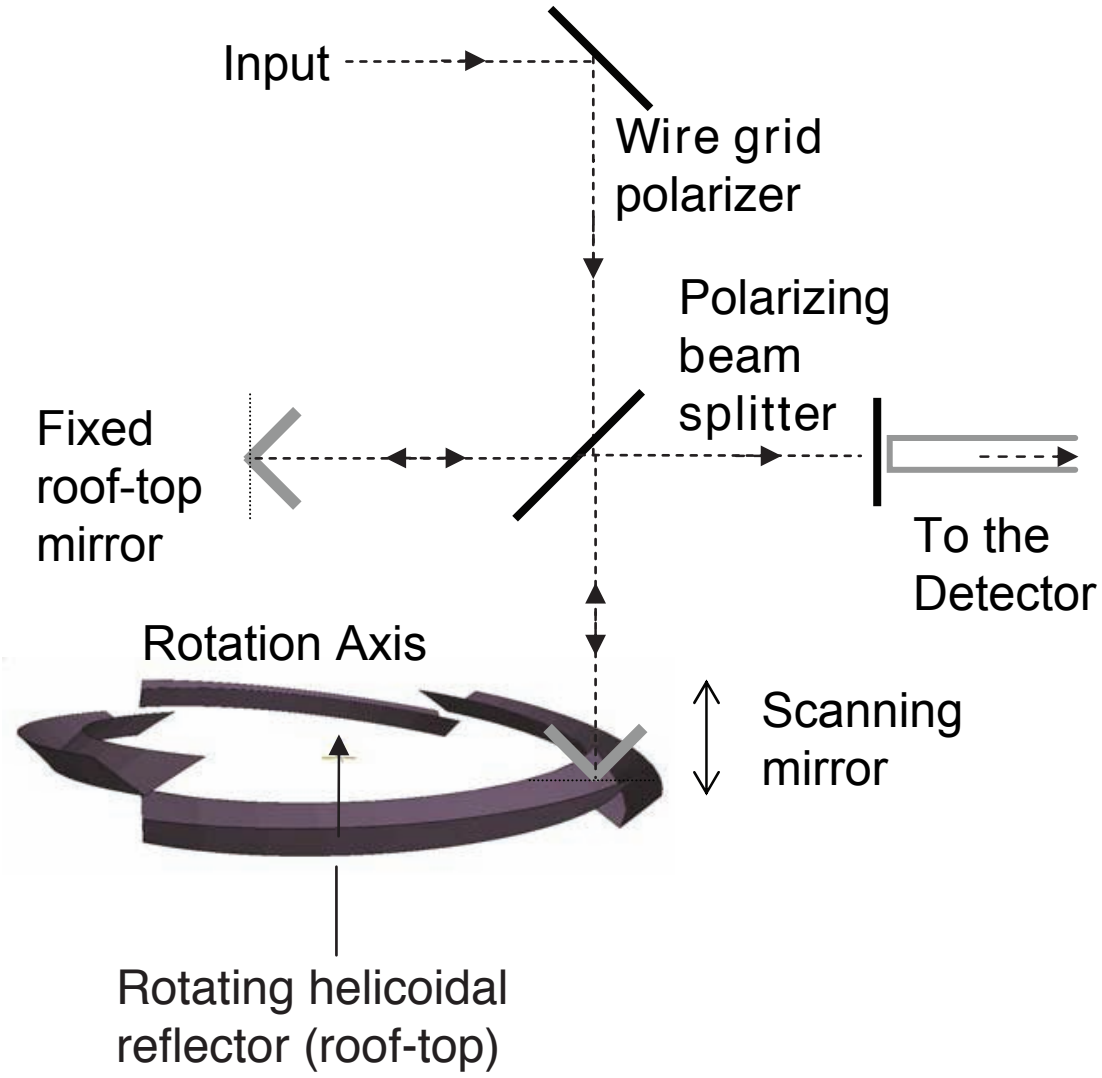

Recent Developments in Electron Cyclotron Emission Research on Magnetically Confined Plasmas / Gary Taylor / Figure 2

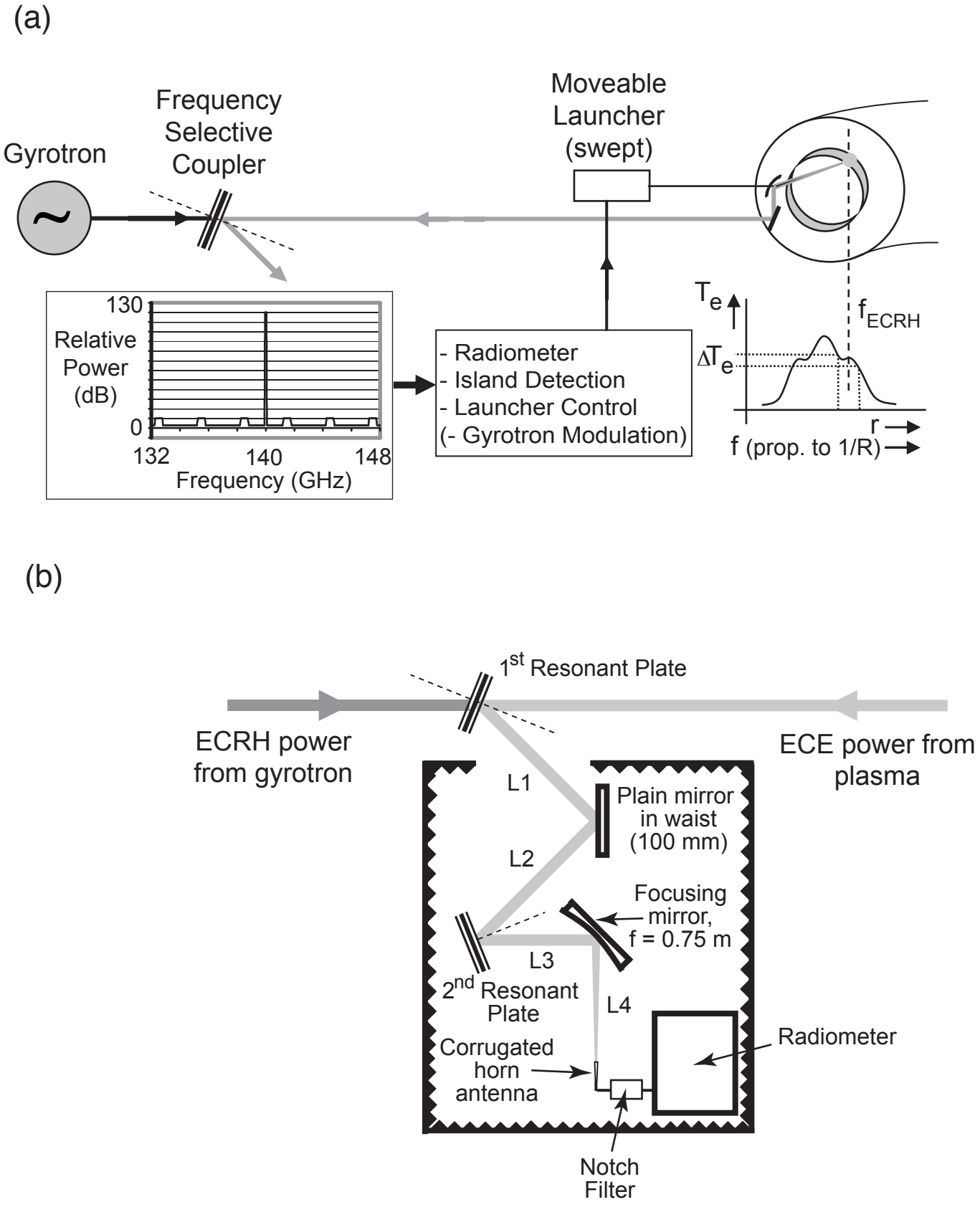

Recent Developments in Electron Cyclotron Emission Research on Magnetically Confined Plasmas / Gary Taylor / Figure 3

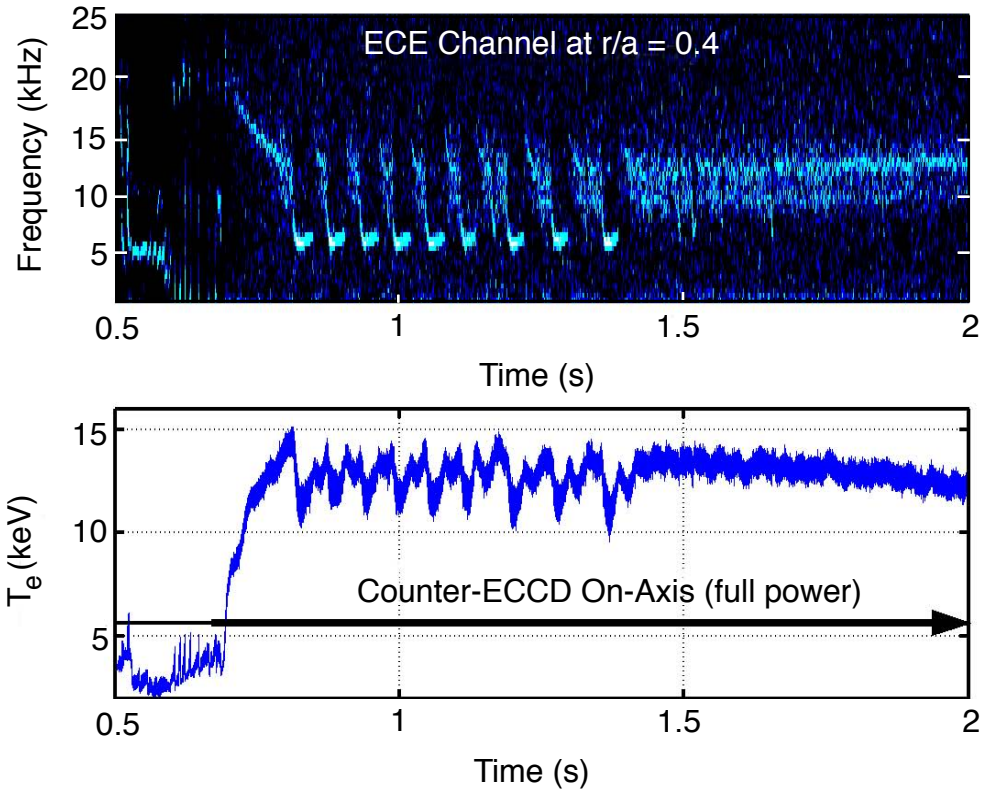

Recent Developments in Electron Cyclotron Emission Research on Magnetically Confined Plasmas / Gary Taylor / Figure 4

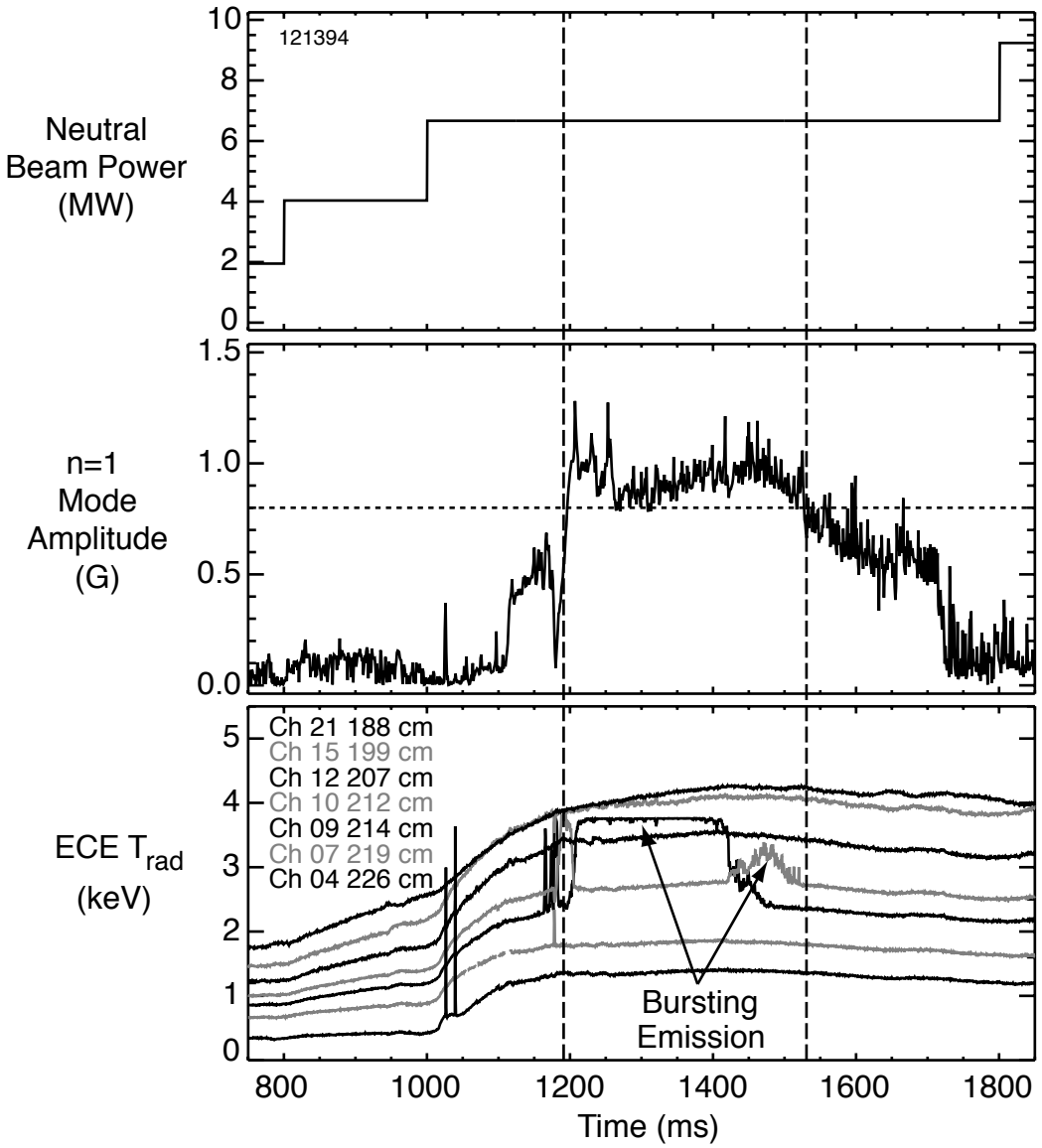

Recent Developments in Electron Cyclotron Emission Research on Magnetically Confined Plasmas / Gary Taylor / Figure 5

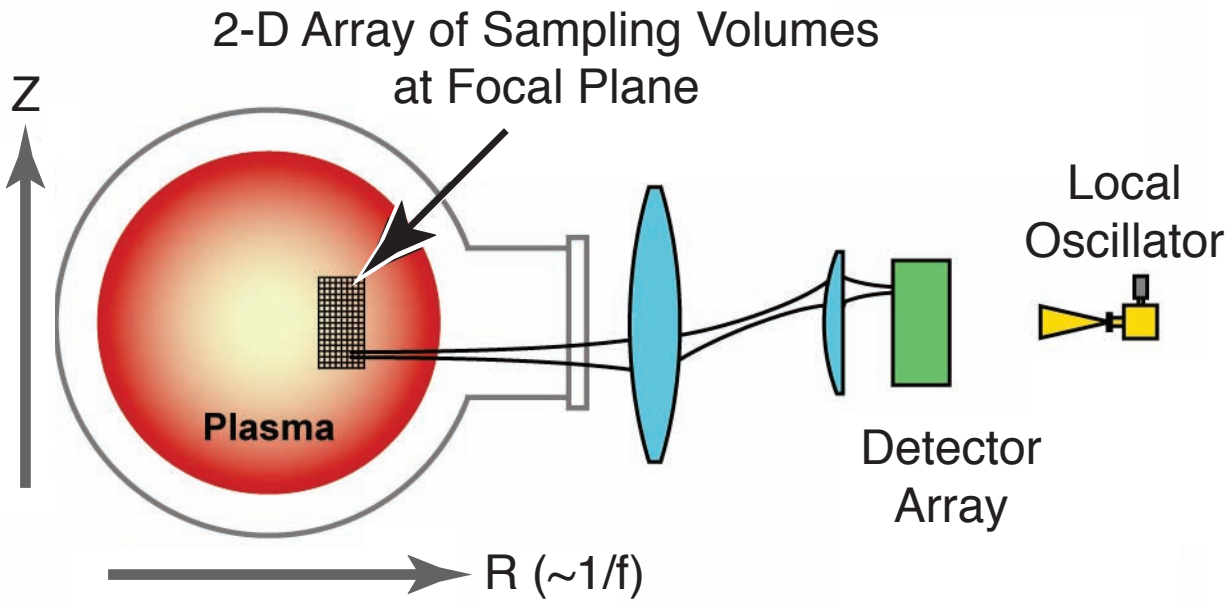

Recent Developments in Electron Cyclotron Emission Research on Magnetically Confined Plasmas / Gary Taylor / Figure 6

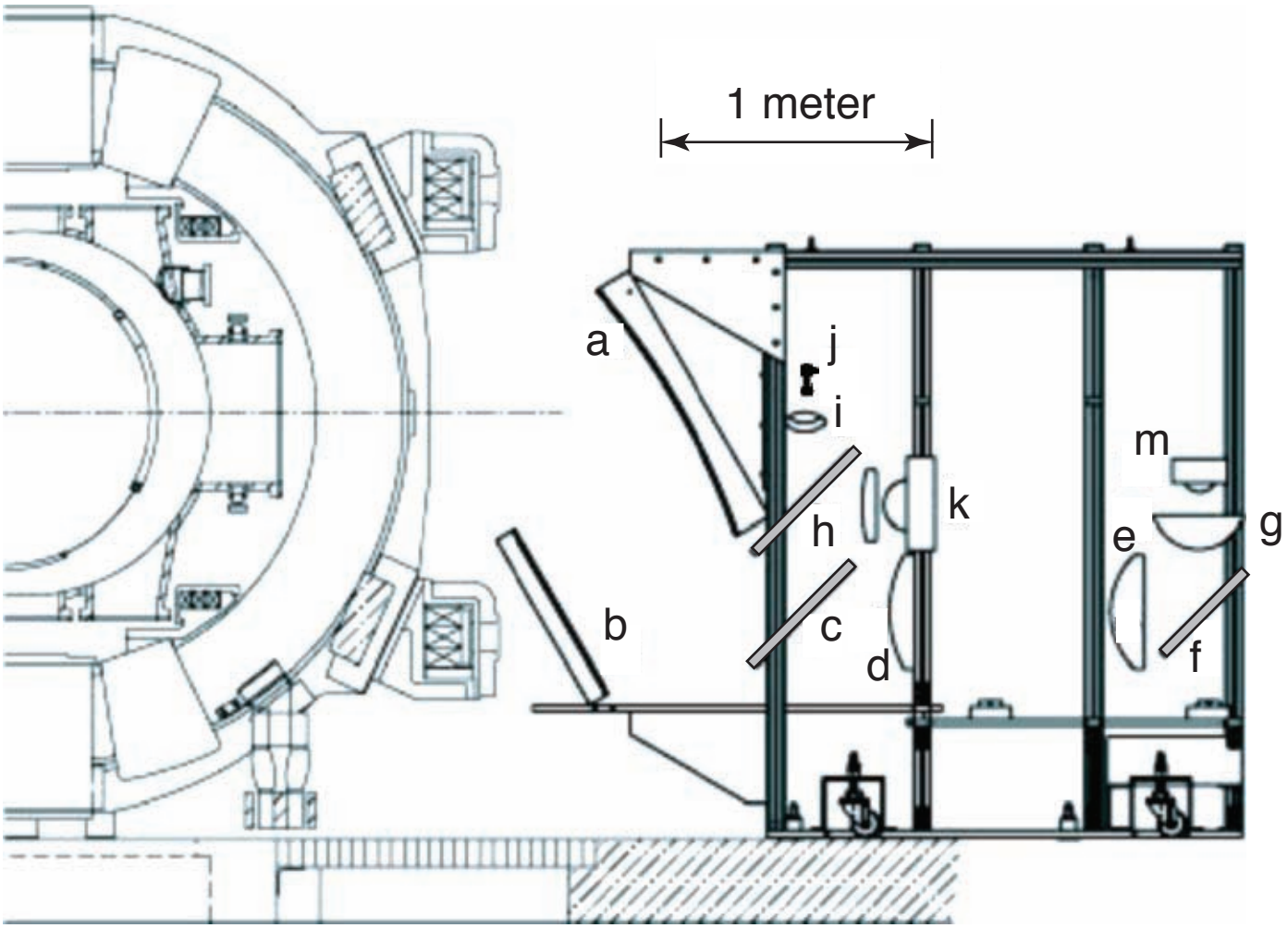

Recent Developments in Electron Cyclotron Emission Research on Magnetically Confined Plasmas / Gary Taylor / Figure 7

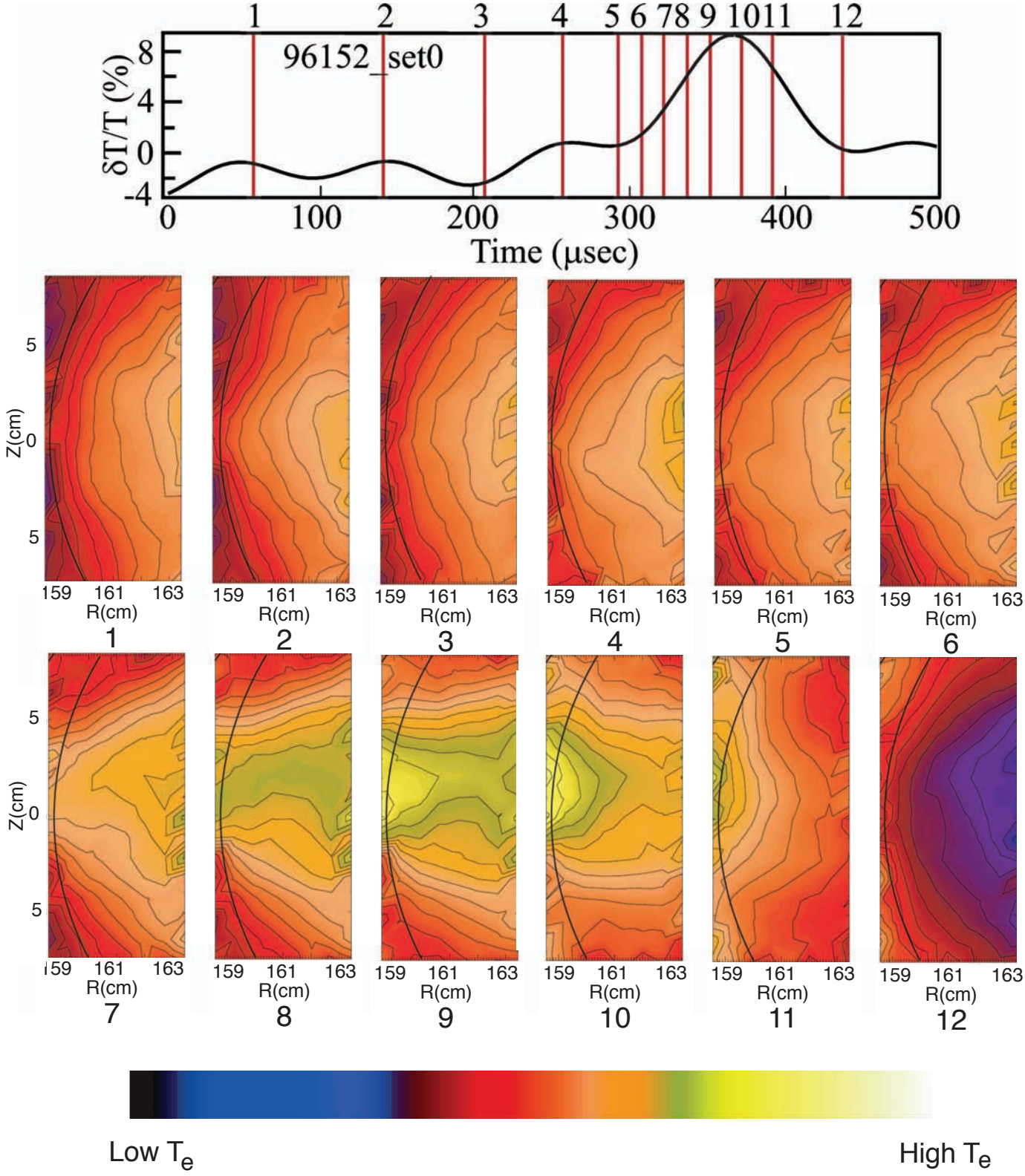

Recent Developments in Electron Cyclotron Emission Research on Magnetically Confined Plasmas / Gary Taylor / Figure 8

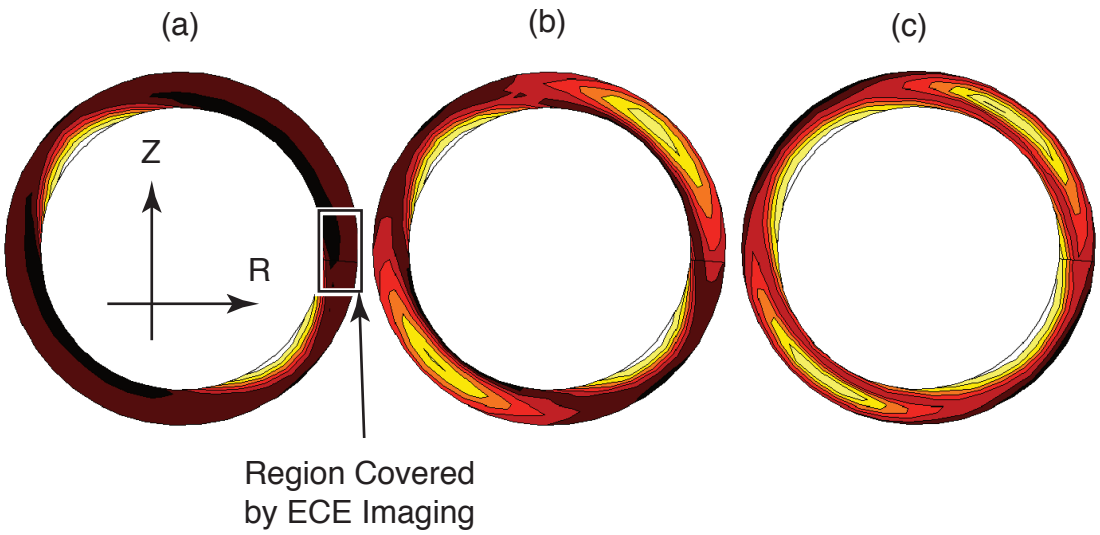

Recent Developments in Electron Cyclotron Emission Research on Magnetically Confined Plasmas / Gary Taylor / Figure 9

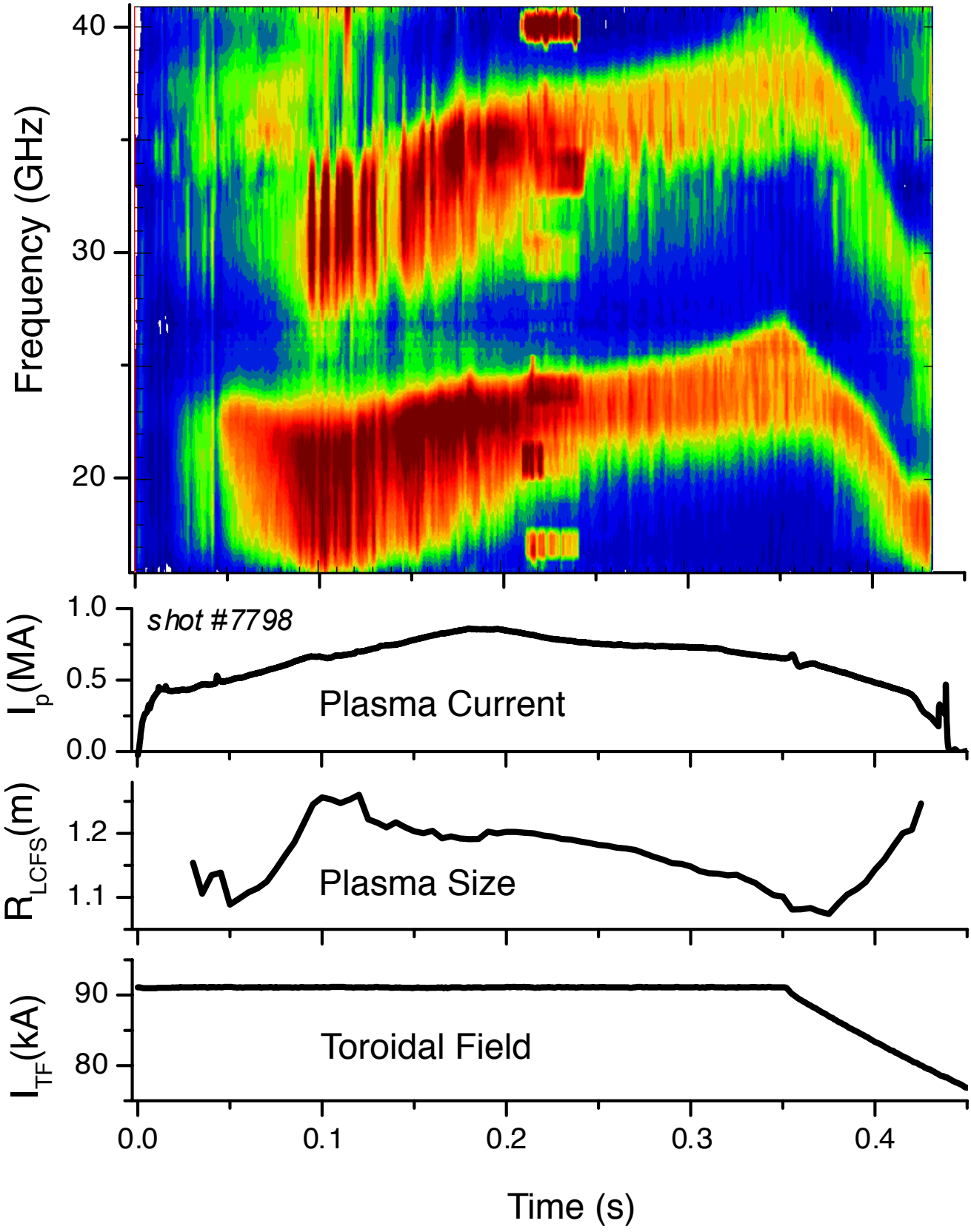

Recent Developments in Electron Cyclotron Emission Research on Magnetically Confined Plasmas / Gary Taylor / Figure 10

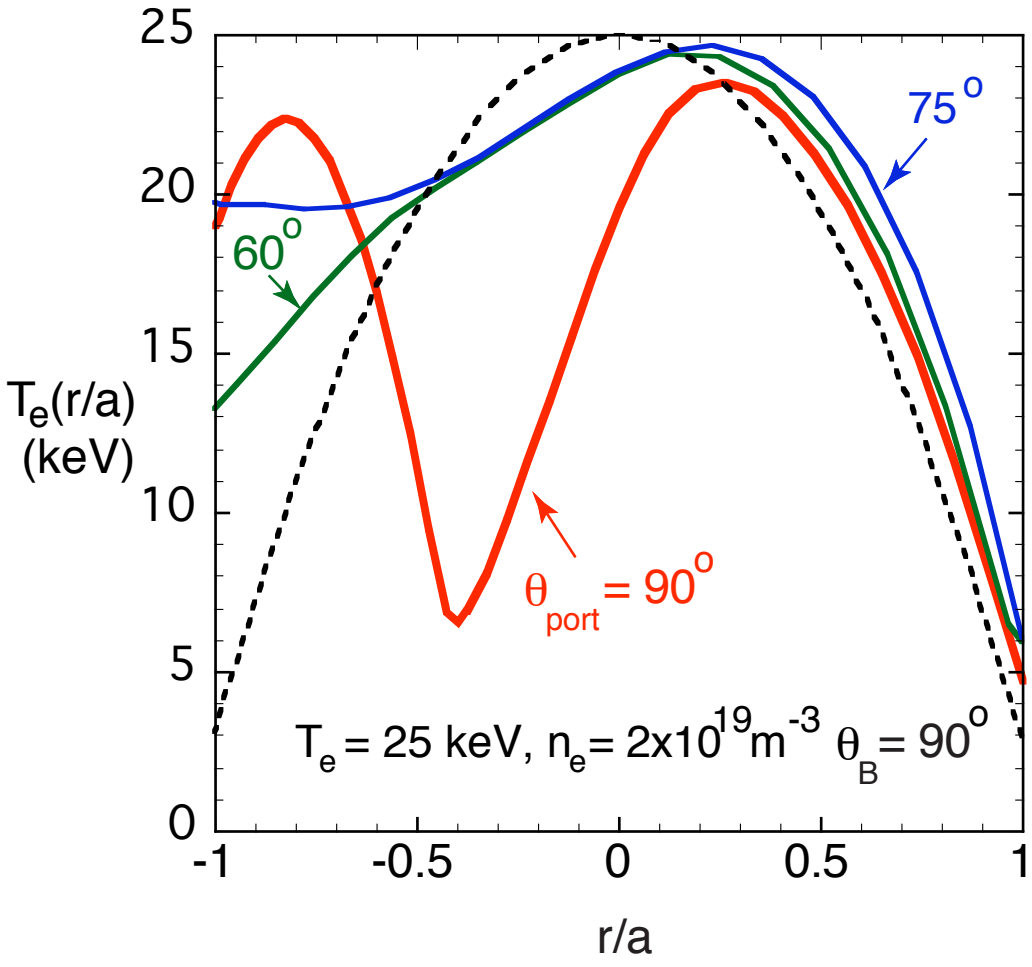

Recent Developments in Electron Cyclotron Emission Research on Magnetically Confined Plasmas / Gary Taylor / Figure 11

The Princeton Plasma Physics Laboratory is operated
by Princeton University under contract
with the U.S. Department of Energy.

Information Services
Princeton Plasma Physics Laboratory
P.O. Box 451
Princeton, NJ 08543

Phone: 609-243-2750
Fax: 609-243-2751
e-mail: pppl_info@pppl.gov
Internet Address: http://www.pppl.gov